Capillary-dominated electrified jets of a viscous leaky dielectric liquid

S. N. Reznik and E. Zussman*
Faculty of Mechanical Engineering, Technion–Israel Institute of Technology, Haifa 32000, Israel
(Received 4 November 2009; published 24 February 2010)

The capillary-dominated regime of dynamics of electrified jets of a viscous leaky dielectric liquid is studied numerically. In this regime the effective force in the direction of an applied field due to tangential electric stresses is balanced by the gradient of liquid pressure governed by the surface-tension stresses. As is characteristic of this regime, the electric current and the characteristic jet radius are dependent on the surface-tension coefficient and not on viscosity. In the scope of this work, the conditions of the existence of this regime are determined. A qualitative order-of-magnitude analysis gives the power-law dependences of the jet radius and electric current on the parameters of the problem (conductivity, applied electric field, flow rate, and surface-tension coefficient). Numerical results are obtained for low conductive liquids for a large range of the dimensionless flow rate (capillary number, Ca). The order-of-magnitude estimations of electric current are in agreement with the numerical results given a small Ca. The corresponding numerically obtained jet shapes are discussed and explained.

DOI: 10.1103/PhysRevE.81.026313 PACS number(s): 47.55.nb, 47.65.−d, 02.60.−x

I. INTRODUCTION

The phenomenon of jetting can be observed in the electrospinning method used for the fabrication of the polymer nanofibers [1–7] or that of electrospraying used for the production of fine sprays of charged drops with nanoscale diameters [8–15]. In these processes, a conducting liquid (in the case of electrospinning, a polymer solution) is supplied from a capillary tube into a region where a capacitorlike electric field exists. If the electric field is sufficiently strong, a stationary liquid jet is observed up to a large distance from the capillary exit. Only small asymmetric distortions of the jet radius exist initially; however these perturbations increase as a result of convective instability (a varicose mode) or bending instability [1–3,6]. In the first case (electrospraying) the liquid can disintegrate into small drops at the conical tip [16,17] or from the ejected jet [15,18]. In the second case (electrospinning) stretching of the bended sections of the jet occurs, the solvent eventually evaporates and as-spun fibers of submicron range diameters are deposited on a counterelectrode. In order to predict the size and charge of the drops obtained by electrospraying or diameters of the fibers obtained by electrospinning it is important to study the characteristics of the stationary jet region, in particular—the electric current flow through the jet for a given applied electric field. By adjusting the rheological and electrical parameters of the liquid, the flow rate and the strength of the applied electric field, it is possible to control the properties of the obtained fibers or droplets. This problem represents a high degree of complexity due to the number of parameters involved, which can result in a wide variety of electrified jet shapes.

Stationary jets of a liquid with large but finite conductivity emitted from an infinite Taylor's cone [19] have been the subject of a number of studies [20–22]. It was shown that for sufficiently high flow rates, the electric current is $I \sim (\gamma K Q)^{1/2}$ (Q is volumetric flow rate, γ is surface-tension coefficient, and K is liquid conductivity). The observation that the electric current depends on γ is to be expected since at a large distances r from the Taylor cone apex the electric field, E_∞ which determines the jet dynamics is on the order of $\sqrt{\gamma/r}$ [19]. Higuera [23] considered the case of jet emission from a small meniscus where the applied electric field is $E_\infty \sim \sqrt{\gamma/a_0}$ (a_0 is the meniscus radius, see Fig. 1). In this case the current or flow rate dependence differs from $O(Q^{1/2})$ due to the finite size of the meniscus. A general scaling theory, limited for high conductive liquids, was suggested by Ganan-Calvo [24] for electrospraying. In all the considered

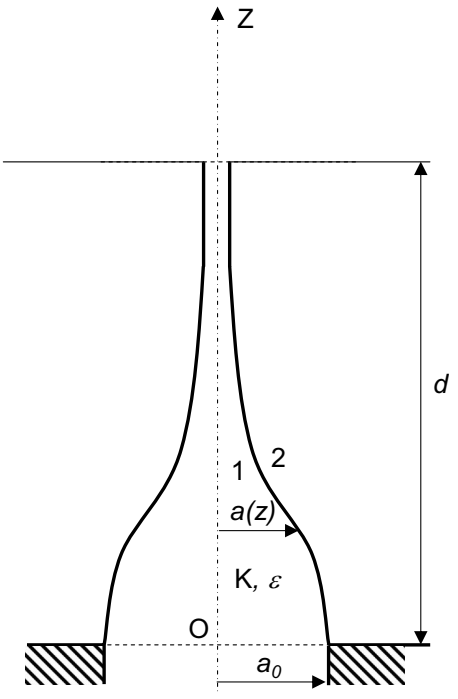

FIG. 1. Sketch of a stationary jet of a leaky dielectric issuing from the orifice in a plane electrode and going toward a counter electrode.

*Corresponding author; meeyal@tx.technion.ac.il

cases the electrical current was not dependent on the applied voltage between the electrodes.

Another situation is realized for jets of viscous low conductivity liquids where a uniform electric field, E_∞ is applied. Numerical calculations and order of magnitude estimations derived for this case show that the current is proportional to $\mu^{1/6}K^{1/2}E_\infty^{2/3}Q^{2/3}$ (μ is liquid viscosity) [25]. Thus, the current is dependent on E_∞ (or the applied voltage, $V=E_\infty d$) and not on γ. This result is clearly only valid for sufficiently high viscosities, high flow rates, and large electric fields when the surface-tension stresses are small in comparison with the viscous and the electric stresses. Electrified jets with these parameters were identified by Higuera [25] as viscosity-dominated jets.

When considering typical parameters used in electrospinning of jets [flow rate $Q \leq 5$ ml/h, $a_0 \sim 1$ mm, $\mu \sim 10$ [g/(cm s)], $\gamma \sim 50$ g/s^2] [4] the capillary number, Ca which determines the relative importance of viscous and surface-tension stresses is found to be $\mathrm{Ca} \sim (\mu Q)/(a_0^2\gamma) \leq 3 \times 10^{-2}$, which is sufficiently small. Hence, surface-tension effects play a significant role in shaping the surface of the jet in the electrospinning process.

The aim of the present work is to study this unexplored regime of jet dynamics, labeled as capillary-dominated and determine its typical conditions. The problem is posed in Sec. II. together with a description of the numerical method. The results are presented and discussed in Sec. III, and the conclusions are presented in Sec. IV.

II. PROBLEM FORMULATION

Consider a conductive incompressible viscous liquid with density ρ and viscosity μ, ejected at a constant (time invariant) flow rate Q from an orifice with a radius a_0 located in a metal plate, toward another plate, located at a distance d($d \gg a_0$) (see Fig. 1). Suppose that a constant electric potential V is applied between the plates. Then, far from the liquid boundary, a constant uniform electric field $E_\infty = V/d$, perpendicular to the plates, is created in the space between the plates. The liquid is supposed to be leaky dielectric [26,27], characterized by a finite (moderate) conductivity K and permeability ε_l. The surrounding medium is supposed to be nonconductive and have the permeability ε_m.

Our aim is to determine the stationary axisymmetric jet surface shape, the distribution of electric field along the jet surface, and the electric current for sufficiently low flow rates Q. In this case the fluid motion is inertialess because the Reynolds number $\mathrm{Re} \sim (\rho Q)/(\mu a_0) \ll 1$. Therefore, it is governed by the Stokes equations. The selected length scale in this problem is the radius of the capillary a_0, the velocity scale is the liquid velocity along the capillary $V_0 = Q/(\pi a_0^2)$, the stresses scale is $\mu V_0/a_0$, the scale of the electric field and charge density is E_∞, the scale of the electric potential is $E_\infty a_0$, and the scale of the electric current is $K\pi a_0^2 E_\infty$. Using these scales, the problem is described by the following set of dimensionless mechanical and electric equations and boundary conditions.

The nondimensional Stokes equations for the liquid motion are

$$\nabla \cdot \mathbf{u} = 0, \quad \nabla p = \Delta \mathbf{u}, \tag{1}$$

where p is pressure and $\mathbf{u}$ is the velocity vector. The problem is axisymmetric, such that $\mathbf{u}$ has only two components: the radial v and the axial w. The electric fields in the liquid and the surrounding media can be written as $E^l = \nabla\varphi^l$, $E^m = \nabla\varphi^m$, respectively, where φ^l, φ^m are the corresponding electric potentials, which in the absence of the volume free charge density satisfy the Laplace equations

$$\Delta\varphi^m = 0, \quad \text{for } r > a(z), \quad \Delta\varphi^l = 0, \quad \text{for } r < a(z), \tag{2}$$

where r, z are the radial and axial coordinates respectively, $a(z)$ describes the jet surface, and Oz is located on the axis of symmetry of the jet (see Fig. 1). Because the jet is stationary, the normal velocity at the free surface of the jet vanishes, and the corresponding kinematic boundary condition is $u_n = 0$ at $r = a(z)$. At the capillary exit, the distribution $w(r,0)$ should satisfy the condition of constant flow rate $\int_0^1 w(r,0)dr = 1$. The dimensionless dynamic boundary conditions at the jet surface are given by

$$f_n = \frac{1}{\mathrm{Ca}}(\kappa + \mathrm{Bo}_E\, f_n^E), \quad f_\tau = \frac{\mathrm{Bo}_E}{\mathrm{Ca}} f_\tau^E, \quad r = a(z). \tag{3}$$

Here f_n, f_τ denote the normal and tangential tractions per unit area of the surface, $f_n^E = (\varepsilon_m E_n^{m^2} - \varepsilon_l E_n^{l^2} + (\varepsilon_l - \varepsilon_m)E_\tau^2)/(8\pi)$, $f_\tau^E = \sigma E_\tau$, σ is a free surface charge density, E_τ is a tangential electric field, and E_n^l, E_n^m are the normal components of electric field in the liquid and the medium, respectively (note that Gaussian units are used). The parameter $\mathrm{Bo}_E = a_0 E_\infty^2/\gamma$ is the electric Bond number, and $\mathrm{Ca} = \mu V_0/\gamma$ is the capillary number.

The boundary conditions for the electric variables are

$$\varphi^m = \varphi^l = 0, \text{ at } z = 0, \quad \varphi^m = \varphi^l = -d \text{ at } z = d, \quad \varphi^m \to -z, \text{ if } r \to \infty, \tag{4}$$

$$\varphi^m = \varphi^l, \quad \varepsilon_m E_n^m - \varepsilon E_n^l = 4\pi\sigma, \text{ at } r = a(z). \tag{5}$$

The stationary dimensionless form of the charge conservation law is the following:

$$I = I_c(z) + I_s(z), \quad I_c(z) = 2\int_0^{a(z)} E_z^l(r,z)rdr, \quad I_s(z) = \mathrm{Pe}\; a(z)\sigma(z)u_t(z), \tag{6}$$

where I is the time invariant overall electric current which should be determined as part of the solution, I_c and I_s are its conductive and convective parts, and u_t is the velocity component tangential to the jet surface. The parameter $\mathrm{Pe} = 2V_0/(Ka_0)$ is the Péclet number. Because $u_t = 0$ at the orifice boundary (i.e., at $z = 0$) the overall current $I = I_c(0)$.

If the jet slope da/dz is sufficiently small, then Eq. (1) with the boundary conditions (3) can be effectively reduced to a simpler one-dimensional (1D) model. If the expansion of the vertical velocity component to r is

$$w(r,z) = w_0(z) + \frac{1}{2}w_2(z)r^2 + \cdots \tag{7}$$

then for $w_0(z)$ and $a(z)$ the following equations can be obtained [28–33]:

$$\frac{\mathrm{Bo}_E}{\mathrm{Ca}}\left(\frac{df_n^E}{dz} + \frac{2f_\tau^E}{a}\right) + \frac{1}{\mathrm{Ca}}\frac{1}{a^2}\frac{da}{dz} + \frac{3}{a^2}\frac{d}{dz}\left(\frac{dw_0}{dz}a^2\right) = 0, \tag{8}$$

$$w_0 a^2 = 1, \tag{9}$$

with the boundary condition at the capillary exit

$$a(0) = w_0(0) = 1. \tag{10}$$

Equation (8) expresses the axial balance of the forces induced by electric stresses (first term), surface tension (second term), and viscous stresses (third term); Eq. (9) expresses the mass conservation. The coefficient w_2 in expansion (7) is expressed as

$$w_2 = \frac{1}{2}w_{0_{zz}} + \frac{3a_z}{a}w_{0_z} + \frac{\mathrm{Bo}_E}{\mathrm{Ca}}\frac{f_\tau^E}{a}. \tag{11}$$

Expanding the solution of the Laplace Eq. (2) for φ^l in the series $\varphi^l = \varphi_0(z) - r^2\varphi_{0_{zz}}/4 + \cdots$ and using the geometric relation $\mathbf{n} = (1, -a_z)/\sqrt{1+a_z^2}$, we get with the accuracy of a one-dimensional approximation

$$E_\tau \approx E_0 = -\frac{d\varphi_0}{dz}, \quad I_c \approx E_0 a^2, \quad E_n^l \approx -\frac{1}{2a}\frac{dI_c}{dz}, \tag{12}$$

where E_0 is an axial field in the liquid. Then, using Eq. (12), the approximate relation $u_t \approx w_0$ and Eq. (9) the charge conservation law (6) becomes

$$E_0 a^2 + \mathrm{Pe}\frac{\sigma}{a} = I. \tag{13}$$

As was previously demonstrated [2,30,34,35] the following approximate equation for E_0 takes place:

$$E_0(z) = 1 - \ln(\chi)\left[\frac{4\pi}{\varepsilon_m}\frac{d(\sigma a)}{dz} - \frac{\beta}{2}\frac{d^2(E_0 a^2)}{dz^2}\right], \tag{14}$$

where $\chi \sim d/a_0 \gg 1$ and $\beta = \varepsilon_l/\varepsilon_m - 1$.

A reasonable boundary condition to Eqs. (13) and (14) at the orifice is zero free charge density [3]. At a large z, where the jet is thin, the electric field is equal to the applied one. Then,

$$\sigma(0) = 0, \quad E_0 \to 1, \quad \text{if } z \to \infty. \tag{15}$$

The solution of Eqs. (13)–(15) gives a good qualitative description of real distribution of E_0 that can be used for explaining the numerical results.

Far downstream from the capillary the jet thins and reaches an asymptotic regime [25]. In this regime, $I \approx I_s$, and the effective force due to normal electric stresses can be neglected in comparison with the force due to the tangential ones $f_\tau^E \approx \sigma E_0 \approx Ia/\mathrm{Pe}$, thus the solution of Eq. (8) has the following asymptotic forms:

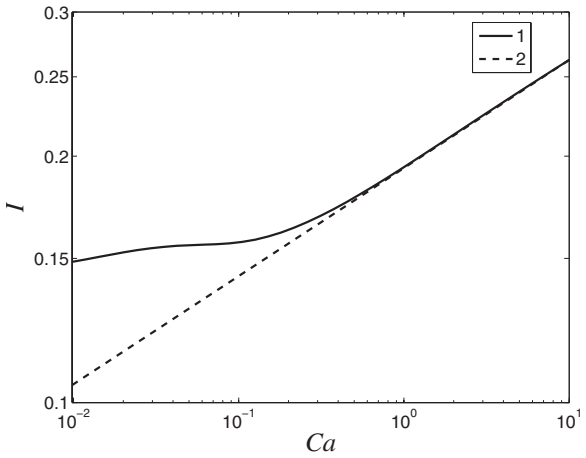

FIG. 2. The dependence of nondimensional electric current I on the capillary number, Ca for the case of $\mathrm{Bo}_E = 1$, $\mathrm{Pe} = 0.2$, $\varepsilon_l = 42.5$, and $\varepsilon_m = 1$ (1), and a power-law dependence $I \sim \mathrm{Ca}^{1/6}$ (2).

$$w_0 \to (kz + c)^2, \quad a \to \frac{1}{kz + c}, \quad k = \frac{1}{12\ \mathrm{Ca}}(\sqrt{1 + 48B} - 1), \quad B = \frac{\mathrm{Bo}_E\ \mathrm{Ca}\ I}{\mathrm{Pe}} \text{ if } z \to \infty, \tag{16}$$

where c is constant. The asymptotic forms in Eq. (16) are to be used as a boundary condition for Eq. (8) at $z = d$ in the numerical calculations.

The procedure for obtaining the numerical solution is as follows. For a fixed initial guess of $a(z)$ the electric stresses f_n^E and f_τ^E and the current I are found by solving the electrical part of the problem. Then, the corrected shape $a(z)$ can be found by solving Eqs. (8) and (9) with boundary conditions (10) and (16), and so on. To find the electric field distribution along the known jetlike surface shape $a(z)$, which is necessary for the determination of the electric stresses, an iterative method was used. Setting an initial surface distribution of $E_n^m(z) = \partial\varphi^m/\partial n|_{r=a(z)}$ the Laplace Eq. (2) with boundary conditions (4) for φ^m in the surrounding media was solved using the boundary element method (BEM) [36–38]. Thus, the conjugated variable distribution $\varphi^m|_{r=a(z)}$ can be found. In the one-dimensional approximation, from the first of the boundary conditions (5) we have $\varphi_0(z) \approx \varphi^m|_{r=a(z)}$ and $E_0(z)$ and $E_n^l(z)$ are known from Eq. (12). The distribution of σ can be found from Eq. (13). Then, the new iteration for $E_n^m(z)$ is found from the second of the boundary condition (5).

III. RESULTS AND DISCUSSION

Numerical results presenting the dependence of the dimensionless electric current, I on the nondimensional viscosity (equivalent to the capillary number, Ca) for $\mathrm{Bo}_E = 1$, and $\mathrm{Pe} = 0.2$, are shown in Fig. 2. The electric current increases with Ca as $I \sim \mathrm{Ca}^{1/6}$ for high Ca, while it converges to a constant for $\mathrm{Ca} \to 0$. The case of high Ca obviously corresponds to the viscosity-dominated regime as explored by Higuera [25], where the opposite case, with low Ca corresponding to a capillary-dominated regime. In the case of capillary-dominated regime, the electric stresses that are act-

ing effectively along the z axis, and stretching the jet, are balanced by the induced surface-tension pressure gradient [the balance of the first two terms in Eq. (8)]. The contribution of the viscous stresses is not ignored, since the tangential electric stresses pulling the liquid along the z axis are balanced by the corresponding tangential viscous stresses which are acting on the jet surface [see Eq. (3)].

To identify an order of magnitude estimate of the electric current for the capillary-dominated regime we consider the transition region, where the conductive current I_c is transferred into convective current, I_s. We label the following parameters in the transition region: the characteristic length of the transition region as z_T, the jet radius as a_T, the axial velocity as $w_T=1/a_T^2$, and the free-surface charge density as σ_T [see Eq. (9)]. Numerical calculations show that the maximal axial electric field in this region is $E_T\sim 1$. Then, by equating $I_s=\mathrm{Pe}\ a_T\sigma_T w_T$ and $I_c=E_T a_T^2\sim a_T^2\sim I$ the following estimates are obtained [25]:

$$a_T\sim I^{1/2},\quad \sigma_T\sim\frac{Ia_T}{\mathrm{Pe}}=\frac{I^{3/2}}{\mathrm{Pe}}. \tag{17}$$

An estimate of z_T can be obtained from the axial force balance [Eq. (8)], where for the case under consideration the last term can be ignored. Then, by equating the first two terms in Eq. (8) we get $1/(a_T z_T)\sim \mathrm{Bo}_E f_\tau^E/a_T$, where $f_\tau^E=\sigma_T E_T \sim Ia_T/\mathrm{Pe}$, and then,

$$z_T\sim\frac{\mathrm{Pe}}{\mathrm{Bo}_E I a_T}\sim\frac{\mathrm{Pe}}{\mathrm{Bo}_E I^{3/2}}. \tag{18}$$

The estimate of the current, I in terms of parameters of the problem can be easily found for sufficiently stretched jets, wherein a_T and I are small. From Eq. (14) it follows that in this case $(\sigma_T a_T)/(\varepsilon_m z_T)\sim 1$ [25]. Then, using estimations (17) and (18) we obtain

$$I\sim\varepsilon_m^{2/7}\mathrm{Pe}^{4/7}\mathrm{Bo}_E^{-2/7}. \tag{19}$$

Its dimensional counterpart is

$$I_{cap}^d\sim\varepsilon_m^{2/7}K^{3/7}E_\infty^{3/7}Q^{4/7}\gamma^{2/7}. \tag{20}$$

Numerical calculations also show that the current decreases with ε_l but this dependence is sufficiently slow. An analogous result was obtained by Pfeifer and Hendrick [16] for pulsating electrospray from capillary and the specific charge of the droplets (charge per unit volume) was found to be

$$q_s\sim\varepsilon_l^{-3/7}\gamma^{2/7}\left(\frac{E_\infty K}{Q}\right)^{3/7}. \tag{21}$$

Then, the current is $I_{cap}^d=Qq_s$, which is similar to Eq. (20). Also in Pfeifer and Hendrick model [16] the viscosity, μ is irrelevant parameter. In their model, it is supposed that droplets are formed by minimizing their total energy (surface and electrostatic). In this case, the droplet charge q is dependent on the droplet radius, R proportionally to the Rayleigh's limit, i.e.,

$$q\sim(\gamma R^3)^{1/2}\quad\text{and}\quad q_s\sim\frac{\gamma^{1/2}}{R^{3/2}}. \tag{22}$$

Comparing Eq. (21) with Eq. (21) and using relations (17) and (19) we get $R\sim a_T^d$, namely the drops in the case of electrospraying, are emitted from the current transfer region near the cone tip. In principle, for the existence of spray of stable drops it is necessary only that $q<(\gamma R^3)^{1/2}$ [39], thus, $R<a_T^d$, meaning that the drops of radius smaller than a_T^d can also eject at a point z^* along the jet, where $a(z^*)<a_T$ (i.e., a point located in the convective region far from the cone tip). The specific charge of the droplets, $q_s=I_{cap}^d/Q$ does not depend on z^* and therefore Eq. (21) is correct also in the considered case of electrospinning.

In the opposite case which Higuera [25] considered, when the capillary effects are negligible, equating the first and third terms in Eq. (8) results in $z_T\sim\mathrm{Ca}^{1/2}\mathrm{Pe}^{1/2}\mathrm{Bo}_E^{-1/2}I^{-1}$ and the resulting current is

$$I\sim\varepsilon_m^{1/3}\mathrm{Pe}^{1/2}\mathrm{Ca}^{1/6}\mathrm{Bo}_E^{-1/6}. \tag{23}$$

Its dimensional counterpart is $I_{vis}^d\sim\varepsilon_m^{1/3}\mu^{1/6}K^{1/2}E_\infty^{2/3}Q^{2/3}$ [25]. Therefore, in the capillary-dominated regime, the electrical current, I_{cap}^d increases with the applied electrical field, as in the case of the viscosity-dominated regime, but more slowly. Contrary to the case of the viscosity-dominated regime, the current is dependent on the surface-tension coefficient, γ and not on the liquid viscosity, μ.

The applicability conditions of the above estimations [Eqs. (19) and (23)] can be obtained from the axial force balance [Eq. (8)]. An estimate of Eq. (19) is correct if the last term (viscous) in Eq. (8) is much smaller than the second term (capillary), namely, $w_T/z_T^2\sim 1/a_T^2z_T^2\ll 1/\mathrm{Ca}a_T z_T$, which can be simplified into $\mathrm{Ca}\ll a_T z_T$. Using estimations (17) and (18) this condition can be written as $B\ll 1$ which is determined in Eq. (16). Analogously, the applicability condition of Eq. (23) is $\mathrm{Ca}\gg a_T z_T$ and can be written as $\sqrt{B}\gg 1$. Thus, the parameter B can be used for determining the type of regime of the jet dynamics.

From Eq. (16) we see that far from the orifice the jet diameter is dependent on B. For $B\leq 0.01$, $k\approx 2B/\mathrm{Ca}$, and therefore $a\approx\mathrm{Pe}/(2\mathrm{Bo}_E I z)$. For $B\geq 1$, $k\approx\sqrt{B/(3\mathrm{Ca}^2)}$ and therefore $a\approx\sqrt{(3\mathrm{CaPe})/(\mathrm{Bo}_E I)}/z$. In the first case, a is not dependent on μ (if I is not dependent on μ), where in the second case a is not dependent on γ (if I is not dependent on γ). Hence, it is reasonable to suppose that for $B\leq 0.01$ the capillary-dominated regime of jet dynamic governs and for $B\geq 1$ the viscosity-dominated regime prevails. An intermediate state takes place, when B lies in the interval $0.01\leq B\leq 1$, where both surface tension and viscosity effects influence the jet shape. Thus, we can predict that Eq. (19) is valid if $B\leq 0.01$, and $I\ll 1$, where Eq. (23) is valid if $B\geq 1$, and $I\ll 1$.

Consider a situation where only the flow rate, Q is varied while the rest of the parameters are fixed. Then, $\mathrm{Pe}=\mathrm{Ca}/q$ and $B=q\mathrm{Bo}_E I$, where $q=(\mu K a_0)/(2\gamma)$ is the ratio of the characteristic hydrodynamic time to the electric relaxation time. Then, the capillary dominated regime is realized if $I\leq 0.01/(q\mathrm{Bo}_E)$ (for $B\leq 0.01$). Since $I\leq 1$ [25] this condition is fulfilled for an arbitrary Ca if $q\leq 0.01/\mathrm{Bo}_E$. For typi-

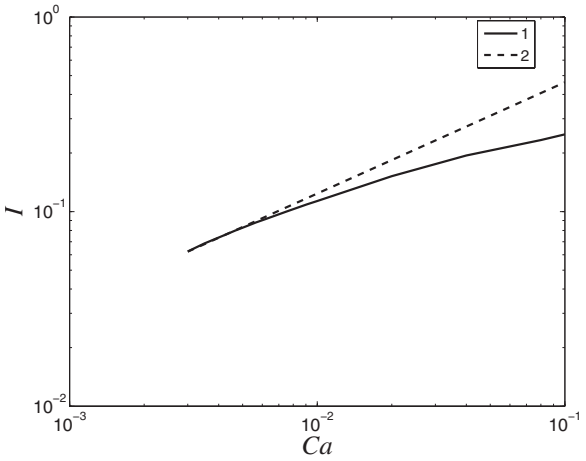

FIG. 3. The dependence of nondimensional electric current I on the nondimensional flow rate Ca for the case $q=(\mu K a_0)/(2\gamma)=0.1$, $\mathrm{Bo}_E=1$, $\varepsilon_l=42.5$, $\varepsilon_m=1$ (1), and a power-law dependence $I \sim \mathrm{Ca}^{4/7}$ (2).

cal parameters of electrospun liquids $\mathrm{Bo}_E \sim 1$, $\mu \sim 10$ g/(cm s), $\gamma \sim 50$ g/s^2, and $a_0 \sim 0.1$ cm [5], we get $K \leq 2$ s^{-1}. This signifies that the capillary-dominated regime is realized, for a large range of flow rates, only for liquids with very low conductivity. For higher conductivities, the capillary-dominated regime exists only for sufficiently small flow rates when I is small. From Eq. (19) it follows that the electrical current $I \sim O(\mathrm{Ca}^{4/7})$ decreases if Ca decreases. Then, we can expect that all the applicability conditions of Eq. (19) are fulfilled if $\mathrm{Ca} \to 0$.

Numerical results presenting the dependence of $I(\mathrm{Ca})$ for the case of $q=0.1$, $\mathrm{Bo}_E=1$, $\varepsilon_l=42.5$, and $\varepsilon_m=1$ are shown in Fig. 3. This dependence is close to $O(\mathrm{Ca}^{4/7})$ for $\mathrm{Ca} \leq 0.007$ which is in a good agreement with the applicability condition $B<0.01$. At higher Ca the current increases more slowly ($I \to 1$ for $\mathrm{Ca} \to \infty$ [25]). The transition to a power-law dependence $O(\mathrm{Ca}^{2/3})$ [see Eq. (23)] is not observed in this graph since for the selected parameters $B \leq 0.1$ and therefore the viscosity-dominated regime is not realized.

Consider the distribution of the electric field along the jet surface for the case corresponding to capillary-dominated regime. The values of the tangential electric field E_0, the outer normal electric field E_n^m, and its components $4\pi\sigma/\varepsilon_m$ and $\varepsilon_l E_n^l/\varepsilon_m$ along the jet for the case of $\mathrm{Bo}_E=1$, $\mathrm{Ca}=0.01$, $\mathrm{Pe}=0.1$, $\varepsilon_l=2$ and 42.5, and $\varepsilon_m=1$ are shown in Fig. 4. In the transition region ($1 \leq z \geq 10$) E_n^m exceeds E_0. In the straight jet section ($z \geq 10$) the opposite relation is realized. We also observe that $E_n^m \approx 4\pi\sigma/\varepsilon_m$ along the entire jet surface when $\varepsilon_l=2$ [see Fig. 4(a)]. In the case of a polar liquid ($\varepsilon_l=42.5$) this relation occurs near the orifice ($z \leq 3$) and far from it ($z \geq 16$). For $3 \leq z \leq 16$ the contribution of E_n^l to the outer normal field E_n^m is on the order of the contribution of the free charge density σ and can even exceed it [see Fig. 4(b)]. This phenomenon can be explained given that near the orifice $I_c = E_0 a^2 \approx I = \mathrm{const}$ and E_n^l is small in accordance with relation (12). For $z \gg 1$, $E_0 \sim 1$, $\sigma \approx Ia/\mathrm{Pe} \sim O(1/z)$, and $E_n^l \approx -a_z \sim O(1/z^2)$ and then $4\pi\sigma \gg \varepsilon_l E_n^l$. In the transition region I_c decreases and E_n^l increases [see Eq. (12)] and its contribution to E_n^m can be significant for large ε_l.

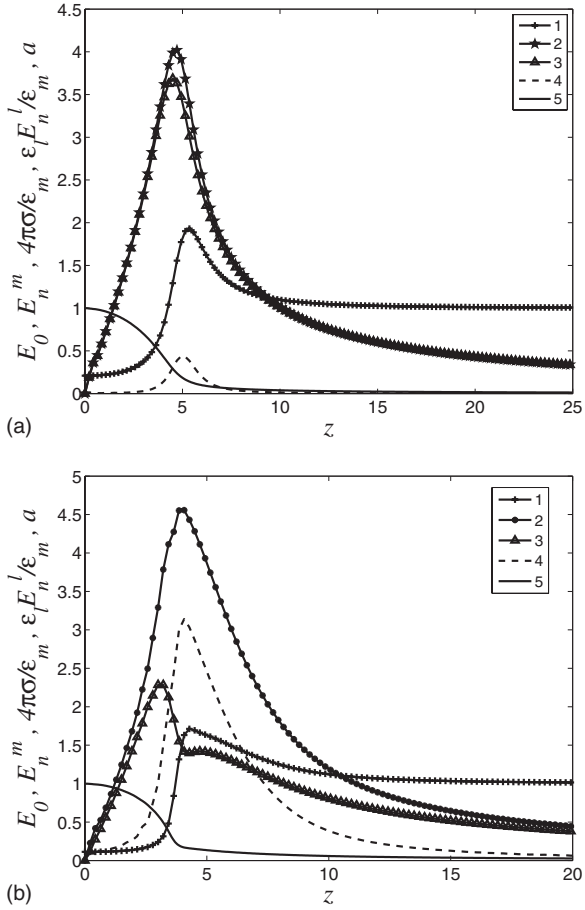

FIG. 4. The distribution of the electric field along the jet surface for the case of $\mathrm{Bo}_E=1$, $\mathrm{Ca}=0.01$, $\mathrm{Pe}=0.1$, and $\varepsilon_m=1$. (1) the tangential field E_0, (2) the outer normal field E_n^m, (3) the component of the outer normal field $4\pi\sigma/\varepsilon_m$, (4) the component of the outer normal field $\varepsilon_l E_n^l/\varepsilon_m$, and (5) the jet shape. (a) Nonpolar liquid with $\varepsilon_l=2$ and (b) polar liquid with $\varepsilon_l=42.5$.

Consider the force balance corresponding to the capillary-dominated regime. The distribution of the terms of Eq. (8) along the z axis, without the viscous term, for polar and nonpolar liquids are presented in Fig. 5. For a polar liquid ($\varepsilon_l=42.5$), we observe that the normal electric stress term, $\mathrm{Bo}_E(df_n^E/dz)$, is balanced by the capillary stress term, $(1/a^2)/(da/dz)$ up to $z \approx 3$ (note that for this case $df_n^E/dz \ll 2f_\tau^E/a$), see Fig. 5(b). This behavior can be explained since in this case $I \ll 1$, hence the axial electric field near the orifice $E_0 \approx I/a^2$ is also small. Then from Eq. (14), taking into account that $\sigma(0)=0$ [see Eq. (15)] we can estimate the free surface charge density as $\sigma \approx (\varepsilon_m z)/[\ln(\chi)a]$. Near the orifice, $a \sim O(1)$, hence, the electric stresses acting on the jet surface in this region can be approximated as

$$f_n^E \approx 2\pi\sigma^2/\varepsilon_m \sim z^2, \quad f_\tau^E \approx \sigma E_0 \sim zI, \tag{24}$$

$df_n^E/dz \gg 2f_\tau^E/a$ for this small I.

For nonpolar liquids ($\varepsilon_l=2$) the electric forces $2f_\tau^E/a$ and df_n^E/dz have the same order of magnitude up to $z \approx 3$ [see Fig. 5(a)] since in this case the current, $I \approx 0.25$ [see Fig. 4(a)] is higher than in the previous case. Far from the orifice,

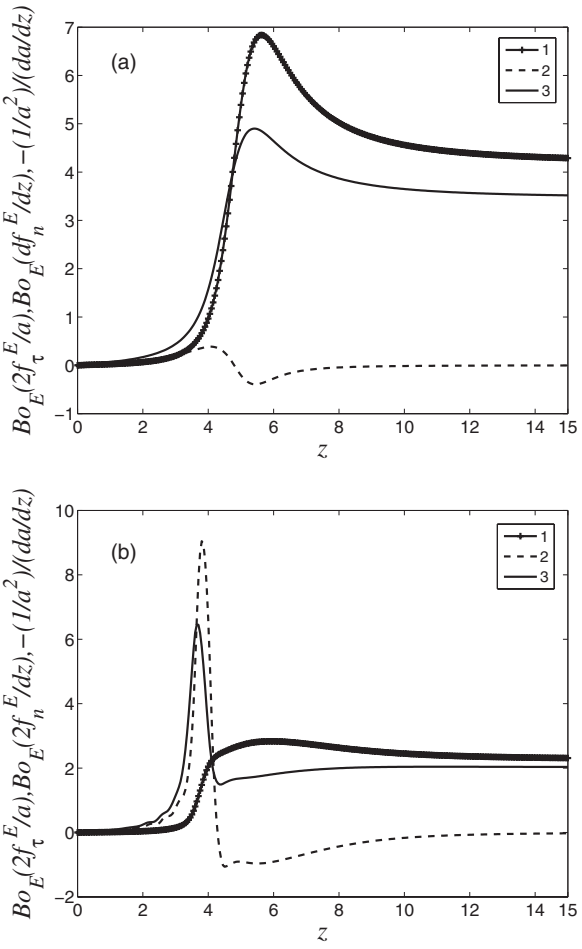

FIG. 5. The dependence of the effective axial forces for the case of $\mathrm{Bo}_E=1$, Ca=0.01, Pe=0.1, and $\varepsilon_m=1$. (1) $\mathrm{Bo}_E(2f_\tau^E/a)$, (2) the term $\mathrm{Bo}_E(df_n^E/dz)$, and (3) the capillary term $-(1/a^2)/(da/dz)$. (a) Nonpolar liquid with $\varepsilon_l=2$ and (b) polar liquid with $\varepsilon_l=42.5$. (Note that for the convenience of presentation, the capillary term is presented with the opposite sign.)

for $z>8$ (see Fig. 5), $df_n^E/dz \ll 2f_\tau^E/a$, and hence the terms $\mathrm{Bo}_E(2f_\tau^E/a)$ and $(1/a^2)/(da/dz)$ balance each other (the existing difference between them is due to the contribution of the small viscous term).

The characteristic shapes of the electrified jet in the capillary-dominated regime with $0.0063<\mathrm{Ca}\leq 0.018$ and large ε_l are shown in Fig. 6. The slope of the different curves, $a(z)$ is close to zero at $z=0$. The curves change their curvature from negative near the orifice to positive in the straight section of the jet. The jet shape in the region near the orifice is elongated and slightly dependent on Ca, whereas in the straight section of the jet its thickness increases with Ca for a fixed z. The geometry of the jet near the orifice can be explained as follows. In this region of the jet, the influence of the tangential electric stresses can be neglected (see above). Then from Eq. (8) when also the viscous term is neglected using the first boundary condition in Eq. (10), we obtain

$$\frac{1}{a}=\mathrm{Bo}_E\frac{2\pi\varepsilon_m z^2}{\ln(\chi)^2 a^2}+1. \tag{25}$$

From Eq. (23) it follows

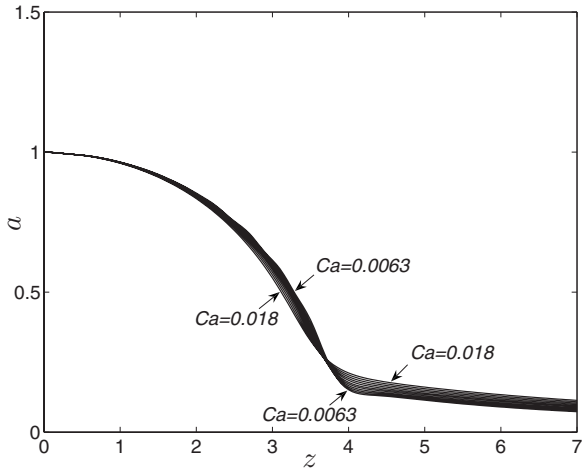

FIG. 6. Jet shapes for the case of $q=(\mu K a_0)/(2\gamma)=0.1$, $\mathrm{Bo}_E=1$, $\varepsilon_l=42.5$, $\varepsilon_m=1$, and different dimensionless flow rate Ca. The flow rate decreases from curve to curve with a factor of 1.1.

$$\frac{da}{dz}(0)=0, \quad \frac{d^2a}{dz^2}(0)=-\frac{4\pi\varepsilon_m}{\ln(\chi)^2}\mathrm{Bo}_E. \tag{26}$$

Since χ is sufficiently large [see Eq. (14)], the curvature near the orifice is small for $\varepsilon_m\sim 1$ and $\mathrm{Bo}_E\sim 1$. This explains the elongated shape of the jet shown in Fig. 6 and also verifies the 1D approximation. The shape of the jet, far from the orifice, in the capillary-dominated regime can be described as $a\sim 1/(kz)\sim \mathrm{Pe}/(\mathrm{Bo}_E I z)$. Using Eq. (19) we can derived $a\sim \varepsilon_m^{-2/7}\mathrm{Pe}^{3/7}\mathrm{Bo}_E^{-5/7}/z$. Subsequently, the jet thickness at a fixed z increases with the flow rate and decreases with conductivity and electric field strength, which is analogous to the case of the viscosity-dominated regime. However, the jet thickness demonstrates a new element in that it increases as a function of the surface-tension coefficient and is independent of the viscosity.

It is interesting to note that although the shape of the inertialess jets far from the orifice is hyperbolic for both the capillary and the viscosity-dominated regimes, the respective profiles of the axial velocity at the jet cross section differ (concave vs convex). From Eq. (11) we have

$$w_2=-5k^2+\frac{\mathrm{Bo}_E I}{\mathrm{CaPe}}, \tag{27}$$

namely, the cross-section profile of the axial velocity is approximately parabolic. From Eqs. (16) and (25) we derive $w_2\approx(\mathrm{Bo}_E I)/(\mathrm{CaPe})>0$ for the capillary-dominated regime ($B\leq 0.01$) and $w_2\approx(-2\mathrm{Bo}_E I)/(3\mathrm{CaPe})<0$ for the viscosity-dominated one ($B\geq 1$). It can be explained as follows. For the capillary-dominated regime from the normal stress balance [Eq. (3)] it follows that at large z the pressure $p\approx -\kappa/\mathrm{Ca}\sim kz/\mathrm{Ca}$ increases linearly with z. Then, the axial velocity profile has a positive curvature for this regime.

IV. CONCLUSIONS

In this paper, the regime of electrospinning of viscous leaky dielectric liquids, wherein jet dynamics is heavily in-

fluenced by capillary effects, was explored numerically. Using a one-dimensional approximate model and qualitative analysis, it was shown that this regime, labeled capillary-dominated, is realized for small values of the dimensionless parameter $B=\mathrm{Bo}_E\mathrm{Ca}I/\mathrm{Pe}$. This is contrary to the previously explored viscosity-dominated regime which is characterized by moderate and high values of B. In the capillary-dominated regime, the jet shape near the orifice is characterized at most by one parameter—the electrical Bond number Bo_E, whereas in the straight jet section the shape also depends on flow rate and the conductivity of the liquid.

The qualitative order-of-magnitude estimations give the power-law dependence of electric current on the parameters of the problem (conductivity, applied electric field, flow rate, and surface-tension coefficient) for the considered regime. This dependence differs from the one obtained for jets issued from Taylor's cone and for the viscosity-dominated regime of jet dynamics. The order-of-magnitude estimations were found to be in good agreement with the numerical results for small capillary numbers.

ACKNOWLEDGMENTS

We gratefully acknowledge the financial support by Russell Berrie Nanotechnology Institute and the U.S.-Israel Bi-National Science Foundation (Grant No. 2006-061).

[1] D. H. Reneker, A. L. Yarin, H. Fong, and S. Koombhongse, J. Appl. Phys. **87**, 4531 (2000).
[2] M. M. Hohman, M. Shin, G. Rutledge, and M. P. Brenner, Phys. Fluids **13**, 2201 (2001).
[3] M. M. Hohman, M. Shin, G. Rutledge, and M. P. Brenner, Phys. Fluids **13**, 2221 (2001).
[4] S. A. Theron, E. Zussman, and A. L. Yarin, Polymer **45**, 2017 (2004).
[5] S. N. Reznik, A. L. Yarin, A. Theron, and E. Zussman, J. Fluid Mech. **516**, 349 (2004).
[6] A. L. Yarin, S. Koombhongse, and D. H. Reneker, J. Appl. Phys. **89**, 3018 (2001).
[7] D. H. Reneker, A. L. Yarin, E. Zussman, and H. Xu, Adv. Appl. Mech. **41**, 43 (2007).
[8] J. Zeleny, Proc. Cambridge Philos. Soc. **18**, 71 (1915).
[9] M. Cloupeau and B. Prunetfoch, J. Electrost. **22**, 135 (1989).
[10] D. Michelson, *Electrostatic Atomization* (Hilger, New York, 1990).
[11] J. F. De la Mora, J. Fluid Mech. **243**, 561 (1992).
[12] A. J. Mestel, J. Aerosol Sci. **25**, 1037 (1994).
[13] A. J. Mestel, Phys. Fluids **14**, 1396 (2002).
[14] A. G. Bailey, *Electrostatic Spraying of Liquid* (Wiley, New York, 1998).
[15] R. T. Collins, J. J. Jones, M. T. Harris, and O. A. Basaran, Nat. Phys. **4**, 149 (2008).
[16] R. J. Pfeifer and C. D. Hendrick, AIAA J. **6**, 496 (1968).
[17] I. Marginean, P. Nemes, and A. Vertes, Phys. Rev. Lett. **97**, 064502 (2006).
[18] A. R. Jones and K. C. Thong, J. Phys. D **4**, 1159 (1971).
[19] G. I. Taylor, Proc. R. Soc. London, Ser. A **280**, 383 (1964).
[20] J. F. De la Mora and I. G. Loscertales, J. Fluid Mech. **260**, 155 (1994).
[21] L. T. Cherney, J. Fluid Mech. **378**, 167 (1999).
[22] F. J. Higuera, J. Fluid Mech. **484**, 303 (2003).
[23] F. J. Higuera, J. Fluid Mech. **513**, 239 (2004).
[24] A. M. Ganan-Calvo, J. Fluid Mech. **507**, 203 (2004).
[25] F. J. Higuera, J. Fluid Mech. **558**, 143 (2006).
[26] J. R. Melcher and G. I. Taylor, Annu. Rev. Fluid Mech. **1**, 111 (1969).
[27] D. A. Saville, Annu. Rev. Fluid Mech. **29**, 27 (1997).
[28] F. J. Garcia and A. Castellanos, Phys. Fluids **6**, 2676 (1994).
[29] V. N. Kirichenko, I. V. Petrianovsokolov, N. N. Suprun, and A. A. Shutov, Dokl. Akad. Nauk SSSR **289**, 817 (1986).
[30] J. J. Feng, Phys. Fluids **14**, 3912 (2002).
[31] J. R. Melcher and E. P. Warren, J. Fluid Mech. **47**, 127 (1971).
[32] A. M. Ganan-Calvo, J. Fluid Mech. **335**, 165 (1997).
[33] A. M. Ganan-Calvo, Phys. Rev. Lett. **79**, 217 (1997).
[34] H. Li, T. C. Halsey, and A. Lobkovsky, Europhys. Lett. **27**, 575 (1994).
[35] H. A. Stone, J. R. Lister, and M. P. Brenner, Proc. R. Soc. London, Ser. A **455**, 329 (1999).
[36] A. A. Becker, *The Boundary Element Method in Engineering: A Complete Course* (McGraw-Hill Companies, New York, 1992).
[37] C. Pozrikidis, *Boundary Integral and Singularity Methods for Linearized Viscous Flow* (Cambridge University Press, Cambridge, 1992).
[38] G. A. L. van de Vorst, Ph.D thesis, Eindhoven University of Technology, 1994.
[39] A. Gomez and K. Q. Tang, Phys. Fluids **6**, 404 (1994).